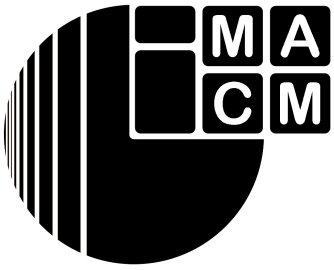

Bergische Universität Wuppertal

Fachbereich Mathematik und Naturwissenschaften

Institute of Mathematical Modelling, Analysis and Computational Mathematics (IMACM)

Preprint BUW-IMACM 20/22

M.W.F.M. Bannenberg, A. Ciccazzo, M. Günther

Coupling of Model Order Reduction and Multirate Techniques for Coupled Dynamical Systems

June 2020

http://www.math.uni-wuppertal.de

Coupling of Model Order Reduction and Multirate Techniques for Coupled Dynamical Systems

M.W.F.M. Bannenberg[a,b], A. Ciccazzo[b], M. Günther[a]

[a] *IMACM, Bergische Universität Wuppertal, Chair of Applied Mathematics and Numerical Analysis (AMNA), Gaußstraße 20, 42119 Wuppertal, Germany.*
[b] *STMicroelectronics, Str. Primsole 50, Catania, Italy*

Abstract

In refined network simulation one is faced with simulating coupled dynamical systems, as for instance circuits are coupled to heat or electromagnetics. Simulation costs of such coupled systems can be reduced by both model order reduction and multirate techniques. In this paper we discuss the coupling of both approaches by linking the slowest first multirate technique to the nonlinear proper orthogonal decomposition model order reduction. For a nonlinear coupled thermal-electrical test example numerical results show the proven convergence of the combined reduced order multirate scheme.

Keywords:
Multirate, Model Order Reduction, Differential-Algebraic Equations, Coupled Systems, Proper Orthogonal Decomposition.

1. Introduction

In time-domain simulation of multiphysical electric circuits, characteristics of the governing set of equations can be exploited: firstly, the multirate (MR) behaviour of the system in the time domain; secondly the vast number of system equations. Previous work [1] regarding the linking of techniques to exploit both characteristics has been done but with respect to linear Model Order Reduction (MOR). In this paper we extend it to the case of differential-algebraic equations (DAEs) coupled to nonlinear ordinary differential equations (ODEs), where the DAEs describe the fast dynamics of electronic circuits, while the ODEs govern slower multiphysical aspects. A twofold approach is presented to efficiently simulate these coupled nonlinear DAEs with first order convergence: by linking the results of [2] to the nonlinear MOR approach of [3] and extended by [4], the differential-algebraic system is reduced and partitioned to be integrated by a reduced order multirate (ROMR) scheme. In the next section we formulate mathematically the dynamical systems to be solved within the multiphysics simulation and, based on that, describe the multirate and MOR techniques. The convergence analysis for our approach is presented in Section 3. Section 4 collects numerical results for a coupled thermal-electric test example. Finally, conclusions are drawn in Section 5.

2. Problem Formulation

This section introduces the preliminaries and definitions needed for the subsequent discussions. In the first part the definition of a coupled dynamical system of DAEs is described, followed by an outline of both POD Q-DEIM model order reduction technique and multirate time integration.

2.1. Coupled multiscale dynamical systems

The dynamics of an electrical circuit is described by DAE network equations, which are analytically equivalent to a semi-explicit DAE of the form, see [5],

$$\dot{y} = \tilde{f}(y,z,t) := f(y,z,u), \quad y(t_0) = y_0, \quad u(t_0) = u_0, \tag{1}$$

$$0 = \tilde{g}(y,z,t) := g(y,z,u), \quad z(t_0) = z_0, \tag{2}$$

with functions $\tilde{f}\colon \mathbb{R}^n \times \mathbb{R}^m \times I \to \mathbb{R}^n$ and $\tilde{g}\colon \mathbb{R}^n \times \mathbb{R}^m \times I \to \mathbb{R}^m$ for the differential and algebraic part, respectively. The quantities $y\colon I \to \mathbb{R}^n$ and $z\colon I \to \mathbb{R}^m$ denote the differential and algebraic variables defined on the time-interval $[t_0, t_1]$, and u couples the network to the PDE model described below. Furthermore y_0 and z_0 need to be consistent initial conditions: for index-1 system assumed in the following, this reads $0 = g(y_0, z_0, u_0)$. Secondly, other phenomena requiring to describe spatial effects can be included via PDEs, which are denoted in general form, given by $\dot{u} = \mathcal{L}(u)$, where $\mathcal{L}$ is a differential operator acting on $u \in D \subset \mathbb{R}^d$, with $d \in \{1, 2, 3\}$ denoting the dimension of the spatial domain. This PDE system is coupled to the DAE system above via boundary conditions, source terms and/or parameters. After applying a suitable space discretization to the PDE system, overall an initial value problem of semi-explicit DAEs is obtained:

$$\dot{y} = f(y, z, u), \quad y(t_0) = y_0, \tag{3}$$
$$0 = g(y, z, u), \quad z(t_0) = z_0, \tag{4}$$
$$\dot{u} = h(y, z, u), \quad u(t_0) = u_0. \tag{5}$$

This system is guaranteed to be of index-1 by the assumption that the Jacobian

$$\frac{\partial g(y, z, u)}{\partial z} \text{ is invertible,} \tag{6}$$

in a neighbourhood of the solution of the system (3-5). From this assumption the algebraic variable z can be solved locally by using the implicit function theorem

$$z = G(y, u). \tag{7}$$

Since the coupled system (3-5) is constructed by the combination of two different processes it can be assumed that they act within different time scales. To exploit this characteristic, the total system is partitioned into fast ($x_F = y$ and $z_F = z$) and slow ($x_S = u$) subsystems,

$$\dot{x}_F = f_F(x_F, z_F, x_S), \quad x_F(0) = x_{F,0}, \tag{8}$$
$$\dot{x}_S = f_S(x_F, z_F, x_S), \quad x_S(0) = x_{S,0}, \tag{9}$$
$$0 = g_F(x_F, z_F, x_S), \quad z_F(0) = z_{F,0}, \tag{10}$$

with $f_F := f, f_S := h$ and $g_f := g$. The subscripts $\{F, S\}$ in the differential variables $x_F \in \mathbb{R}^{n_F} (n_F := n)$, $x_S \in \mathbb{R}^{n_S}$ and algebraic variables $z_F \in \mathbb{R}^{n_Z} (n_Z := m)$ indicate fast or slow dynamics, for $t \in [t_0, t_1]$ with consistent initial conditions. The algebraic constraints are assumed to be fast, as the whole dynamics of the DAE system is fast. This type of coupling lets us consider electrical circuits with a differential index up to 1, coupled to slower ODE systems.

2.2. POD Q-DEIM

Applying a space discretization to the PDE can result in large nonlinear ODE systems. To reduce the computational effort needed to solve this system in each time step MOR techniques are used. Due to the nonlinearity of the ODE most conventional MOR techniques can be discarded as they are tailored to linear systems. Hence the chosen method for this system is a reduction by a Galerkin projection constructed by Proper Orthogonal Decomposition (POD), [6]. This is then extended by the application of the Discrete Empirical Interpolation Method (DEIM), [3], exploiting a QR selection procedure (Q-DEIM), [4]. By using a Galerkin projection a reduced model is constructed, [4], which guarantees that the reduced system is again index 1. Let $V \in \mathbb{R}^{n_S \times r}$ be a non-square matrix with independent columns, with $n_S \gg r$, then $\mathcal{V}_r$ denotes an r-dimensional subspace spanned by these columns. The full state of the slow subsystem x_S is then approximated by $x_S \approx V x_{S,r}$ using the model reduction basis V. The reduced model in the fast unknowns x_F, z_F and slow unknowns $x_{S,r}$ is then defined by

$$\dot{x}_F = f_F(x_F, z_F, V x_{S,r}), \qquad x_F(0) = x_{F,0}, \tag{11}$$
$$\dot{x}_{S,r} = f_{S,r}(x_F, z_F, x_{S,r}), \qquad x_{S,r}(0) = x_{S,r,0}, \tag{12}$$
$$0 = g_F(x_F, z_F, V x_{S,r}), \qquad z_F(0) = z_{F,0} \tag{13}$$

with $f_{S,r}(x_F, z_F, x_{S,r}) = V^T f_S(x_F, z_F, V x_{S,r})$, where the full state is needed for the coupling. The reduction basis V is constructed through POD. First a numerical simulation of the full system (8-10) is performed. From the numerical results of this simulation *snapshots* $\{x_i\}$ are obtained, with x_i for $i = 1, \ldots, N_S$ denoting the numerical approximation of x_S at time point t_i of the full system. Then the POD *snapshot matrix*, for the slow variables only, is defined by

$$\mathbb{X} = [x_1, \ldots, x_{N_S}] \in \mathbb{R}^{n_S \times N_S}. \tag{14}$$

From this the Singular Value Decomposition (SVD) is computed

$$\mathbb{X} = Z \Sigma Y^T, \tag{15}$$

where $Z \in \mathbb{R}^{n_S \times k}$, $Y \in \mathbb{R}^{N_S \times k}$ are orthogonal and $\Sigma = \mathrm{diag}(\sigma_1, \ldots, \sigma_k) \in \mathbb{R}^{k \times k}$ with $k = \min(n_S, N_S)$. Now a reduction basis V can be constructed by taking the leading r singular vectors of Z corresponding to the r largest singular values. However, denote that there is still a problem with the Galerkin projection of the reduced term, $f_{S,r}(x_F, z_F, x_{S,r})$, causing computational inefficiencies. This term has a computational complexity that depends on the non-reduced full order size n_S. To reduce the computational complexity Q-DEIM is applied, [3].

Consider the nonlinear function $f_S : \mathcal{T} \to \mathbb{R}^{n_S}$ with $\mathcal{T} \subset \mathbb{R}^{n_S}$, and matrix $U \in \mathbb{R}^{n_S \times m}$ of rank m. Then the DEIM approximation of f_S is defined by [3, Definition 3.1],

$$\hat{f}_S(\tau) := U(\mathbb{S}U)^{-1}\mathbb{S}^T f_S(x_F(\tau), z_F(\tau), x_S(\tau)), \tag{16}$$

where $\mathbb{S}$ is a selection matrix of size $n_S \times m$ by selecting columns of identity matrix $\mathbb{I}$ of size $n_S \times n_S$. Then the reduced nonlinear function $f_{S,r}$ is approximated with the Q-DEIM, we replace f_S by $f_{S,r}$ (the coupled terms x_F and z_F are dropped here from the notation as these are not reduced)

$$f_{S,r}(x_{S,r}) \approx V^T U(\mathbb{S}U)^{-1}\mathbb{S}^T f_S(V x_{S,r}). \tag{17}$$

Using the interpolation of general nonlinear functions, outlined in [3, Section 3.5], a general nonlinear function can be represented as

$$\big[F(y)\big]_i = F_i(y) = F_i(y_{j_1^i}, y_{j_2^i}, \ldots, y_{j_{n_i}^i}) = F_i\big(y(j_i)\big), \tag{18}$$

where $F_i : \mathcal{Y}_i \to \mathbb{R}$, $\mathcal{Y}_i \subset \mathbb{R}^{n_i}$, with integer vector $j_i = [j_1^i, j_2^i, \ldots, j_{n_i}^i]$ denoting the indices of the components required to evaluate F_i. The numerical implementation of this allows to compute (17) without the full evaluation of f_S.

2.3. Multirate Implicit Euler

The overall index-1 system (11)-(13) can be integrated with the stiffly accurate Implicit Euler scheme, which automatically assures that also for $t > 0$ the quantities will remain consistent. To exploit the assumed different time scales, a multirate integration scheme is proposed. This approach is analogous to [2], but with the algebraic constraint in the fast subsystem, and taking the subsequent MOR into account. The integration of the coupled system (11)-(13) for one macro-step $t_n \to t_{n+1} = t_n + H$ is defined as

$$x_{F,n+(l+1)/m} = x_{F,n+l/m} + h f_F(x_{F,n+(l+1)/m}, z_{F,n+(l+1)/m}, \bar{x}_{S,n+(l+1)/m}), \tag{19}$$

$$x_{S,n+1} = x_{S,n} + H f_{S,r}(\bar{x}_{F,n+1}, \bar{z}_{F,n+1}, x_{S,n+1}), \tag{20}$$

$$0 = g_F(x_{F,n+(l+1)/m}, z_{F,n+(l+1)/m}, \bar{x}_{S,n+(l+1)/m}), \tag{21}$$

with $l = 0, \ldots, m-1$, counting the micro step approximations at the micro grid, where $h = H/m$. The coupling variables are denoted by $\bar{x}_F$, $\bar{z}_F$, $\bar{x}_s$. The coupling strategy is chosen to be the *Coupled-Slowest-First* approach as this is shown to have a consistency of order 1 for the problem posed in [2]. First the whole

system is solved for the macro-step.

$$x^*_{F,n+1} = x_{F,n} + Hf_F(x^*_{F,n+1}, z^*_{F,n+1}, x_{S,n+1}), \tag{22}$$

$$x_{S,n+1} = x_{S,n} + Hf_{S,r}(x^*_{F,n+1}, z^*_{F,n+1}, x_{S,n+1}), \tag{23}$$

$$0 = g_F(x^*_{F,n+1}, z^*_{F,n+1}, x_{S,n+1}). \tag{24}$$

The step size H is chosen according to the slow dynamics, whilst the full system remains solvable. From this it follows that the fast solutions, $x^*_{F,n+1}$ and $z^*_{F,n+1}$, are not accurate enough and can be discarded, as they will be computed in the last micro step. In a second step, the fast solutions are computed for the micro steps $l = 0, \ldots, m-1$, using for the interpolated values $\bar{x}_{S,n+(l+1)/m}$ linear interpolation based on the available information $x_{S,n}$ and $x_{S,n+1}$in time values for the slow variables.

3. Numerical Analysis

Let $y_{\{\text{full,red}\}} \colon [t_0, t_{\text{end}}] \to \mathbb{R}^k$ denote all the variables of the full system (8)–(10) and of the reduced system (11)–(13), respectively. Let the exact values be denoted with $y(t)$ for t in the interval $[t_0, t_n]$. Furthermore, let y_n denote the numerical approximation after n macro-steps. Let $||\cdot||$ denote the 2-norm in Euclidean space. To numerically integrate the reduced order system (11)-(13) with a ROMR scheme we are interested in the difference between the numerical approximation computed by the reduced multirate scheme and the exact solution of the full order model.

$$\left\| y_{\text{full}}(t_{n+1}) - \tilde{V} y_{\text{red},n+1} \right\|, \tag{25}$$

where $\tilde{V}$ is the orthonormal projection matrix for the full system, defined as

$$\begin{pmatrix} I & 0 & 0 \\ 0 & V & 0 \\ 0 & 0 & I \end{pmatrix}. \tag{26}$$

Here V is the projection of the slow part, the other quantities are not reduced. We split the approximation errors into two parts, the reduction error and the numerical error.

$$\left\| y_{\text{full}}(t_{n+1}) - \tilde{V} y_{\text{red},n+1} \right\| \leq \left\| y_{\text{full}}(t_{n+1}) - \tilde{V} y_{\text{red}}(t_{n+1}) \right\| - \left\| \tilde{V} y_{\text{red}}(t_{n+1}) - \tilde{V} y_{\text{red},n+1} \right\|. \tag{27}$$

By using [7, Theorem 4.2], we have that

$$\int_0^{t_{n+1}} \left\| y_{\text{full}}(t) - \tilde{V} y_{\text{red}}(t) \right\|^2 dt \leq C(t_{n+1})(\mathcal{E}_y + \mathcal{E}_F), \tag{28}$$

where $C(t_{n+1})$ is the magnification factor, and $\mathcal{E}_y$ and $\mathcal{E}_F$ are the 2-norm errors from approximating the solution $y_{\text{full}}(t)$ with POD and the nonlinear function with Q-DEIM. Now we have that $\left\| y_{\text{full}}(t) - \tilde{V} y_{\text{red}}(t) \right\|^2$ is a Riemann integrable function and thus it holds that

$$\int_0^{t_{n+1}} \left\| y_{\text{full}}(t) - \tilde{V} y_{\text{red}}(t) \right\|^2 dt \leq C(t_{n+1})(\mathcal{E}_y + \mathcal{E}_F) \implies \left\| y_{\text{full}}(t_n) - \tilde{V} y_{\text{red}}(t_n) \right\|^2 \leq \tilde{C}(t_{n+1})(\mathcal{E}_y + \mathcal{E}_F), \tag{29}$$

where $\tilde{C}(t_{n+1}) = \frac{1}{t_n} C(t_{n+1})$, following the upper and lower bound inequality of Riemann integrals. For the bound of the numerical error from Equation (27) we first observe that obtaining the fast algebraic approximates via the implicit function theorem and via the implicit Euler method are the same, as the implicit

Euler method is stiffly accurate and thus automatically consistent. Therefore the numerical approximation error in the algebraic variable only depends on y_F and y_{S_r}:

$$z_{F,n+\frac{1}{m}} - z_F(t_{n+\frac{1}{m}}) = G(y_{F,n+\frac{1}{m}}, y_{S_r,n+\frac{1}{m}}) - G(y_F(t_{n+\frac{1}{m}}), y_{S_r}(t_{n+\frac{1}{m}})). \tag{30}$$

This is equal to the case c in, [2, Lemma 2]. Therefore, [2, Theorem 2], can be applied which gives that the numerical error

$$\left\| \tilde{V} y_{\text{red}}(t_{n+1}) - \tilde{V} y_{\text{red},n+1} \right\| \approx \mathcal{O}(H), \tag{31}$$

where H is the macro step-size of the mrIRK-DAE1 scheme. From this it follows that the reduced order multirate global approximation error is given by

$$\left\| y_{\text{full}}(t_{n+1}) - \tilde{V} y_{\text{red},n+1} \right\| \approx \sqrt{\tilde{C}(t_{n+1})(\mathcal{E}_y + \mathcal{E}_F)} + \mathcal{O}(H). \tag{32}$$

Thus if the reduction error is chosen such that

$$\sqrt{\tilde{C}(t_{n+1})(\mathcal{E}_y + \mathcal{E}_F)} = \mathcal{O}(H) \tag{33}$$

the method converges with order 1 in H to a solution which is within $\mathcal{O}(H)$ distance of the full solution. This small choice is always possible as the bound can be made arbitrarily small. One caveat could be that if the system is unsuitable for reduction, the reduction error will only be small for a small dimension reduction. Then this will not lead to improved computational times as the system will not be sufficiently reduced and the large projections can increase the computational effort. However, our thermal-electrical benchmark perfectly allows for reduction.

4. Numerical Results

This section verifies the convergence results obtained in the previous section numerically by applying the reduced order multirate scheme to a test problem. As the test circuit needs to contain both coupling and different intrinsic time scales, the thermal-electric test circuit as described in [8] is used, Figure 1. This circuit consists of an operational amplifier, two resistors, a diode and a capacitor. The resistor $R(T)$

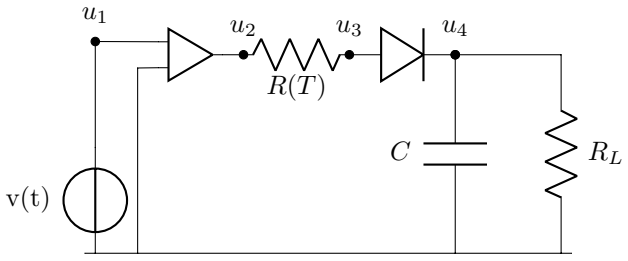

Figure 1: Electric description of the benchmark circuit.

produces and transports heat and is temperature dependent. The amplifier is a heat source and the diode has a temperature dependent characteristic curve. The electric behaviour of the circuit is modelled by nodal analysis yielding from Kirchhoff's laws. Following the discretisation as done in [8] we arrive at the following thermal-electric system:

Electric network:

$$\begin{aligned} 0 &= (Av(t) - u_3)/R(T) + i_{di}(u_3 - u_4, T_{di}), \\ C\dot{u}_4 &= i_{di}(u_3 - u_4, T_{di}) - u_4/R_L, \end{aligned}$$

Coupling interfaces:

$$P_{op} = |(v_{op} - |v(t)| \cdot (Av(t) - u_3)/R|, \quad P_w = (Av(t) - u_3)^2/R,$$

$$R(T) = \left(\frac{1}{2}(\rho(0, T_0) + \sum_{i=1}^{N-1} \rho(X_i, T_i) + \frac{1}{2}\rho(l, T_N)\right) \cdot h,$$

Heat equation:

$$M'_{w,i} h \dot{T}_i, = \Lambda \frac{T_{i+1} - 2T_i + T_{i-1}}{h} + P_w \frac{\tilde{\rho}(X_i, T_i)}{R} h - \gamma S'_{w,i} h (T_i - T_{env}), \quad (i = 1, ..., N-1),$$

$$(M'_{w,0} \cdot \frac{h}{2} + M_{op}) \dot{T}_0 = \Lambda \frac{T_1 - T_0}{h} + P_w \frac{\tilde{\rho}(0, T_0)}{R} \frac{h}{2} - \gamma (S'_{w,0} \frac{h}{2} + S_{op}) \cdot (T_0 - T_{env}) + P_{op},$$

$$(M'_{w,N} \cdot \frac{h}{2} + M_{di}) \dot{T}_N = \Lambda \frac{T_{N-1} - T_N}{h} + P_w \frac{\tilde{\rho}(X_N, T_N)}{R} \frac{h}{2} - \gamma (S'_{w,N} \frac{h}{2} + S_{di}) \cdot (T_N - T_{env})$$

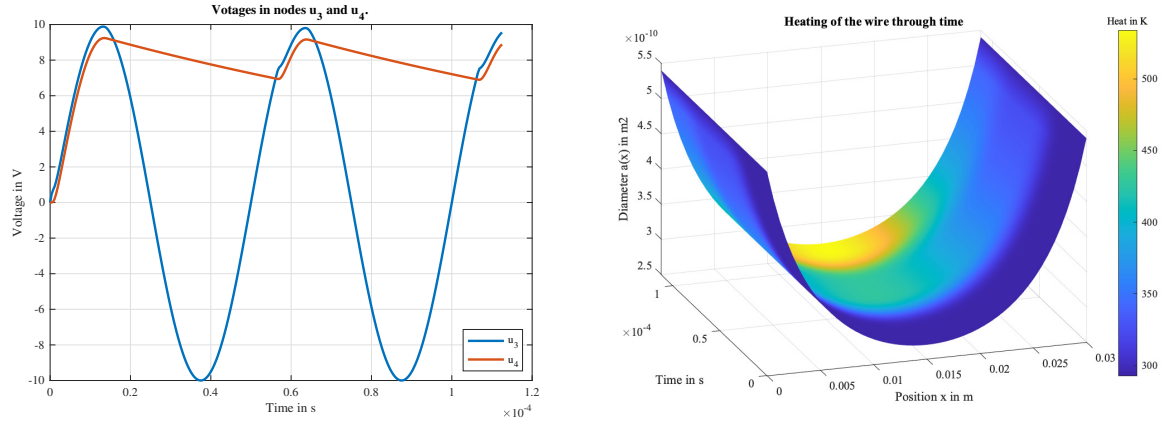

Figure 2: Full system solution, consistent with [8] (left), heat flow in time through the resistor (right).

The coupled thermal-electric system is simulated over the time interval $[0\ 1.125 \cdot 10^{-4}]$. The thermal PDE is spatially discretized into $N = 1000$ voxels. The model is reduced such that $\frac{\sigma_{r+1}}{\sigma_1} < 1 \cdot 10^{-15}$. In Figure 2 the evolution of the thermal electrical system through time is shown. To assess the error of the ROMR scheme the obtained voltages at nodes u_3 and u_4 are compared to a highly accurate reference solution. Figure 3 shows this comparison for the single rate (SR) scheme, the MR scheme and the ROMR scheme. It shows that the reduced order multirate scheme error, the left figure, follows the $\mathcal{O}(H)$ convergence rate in both the algebraic, u_3, and dynamic, u_4, variables. In the right figure, it shows the computation time versus the difference with the reference solution.

5. Conclusion and Outlook

The multirate time integration scheme has successfully been extended to incorporate model order reduction methods. The resulting reduced order multirate scheme is guaranteed to be consistent and converges with order 1. The numerical results obtained for the test example confirmed these analytical results and showed that the reduced order multirate scheme can be successfully applied to coupled dynamical systems. Further research will be conducted by applying a reduced order multirate scheme to a coupled dynamical system composed of two differential algebraic systems.

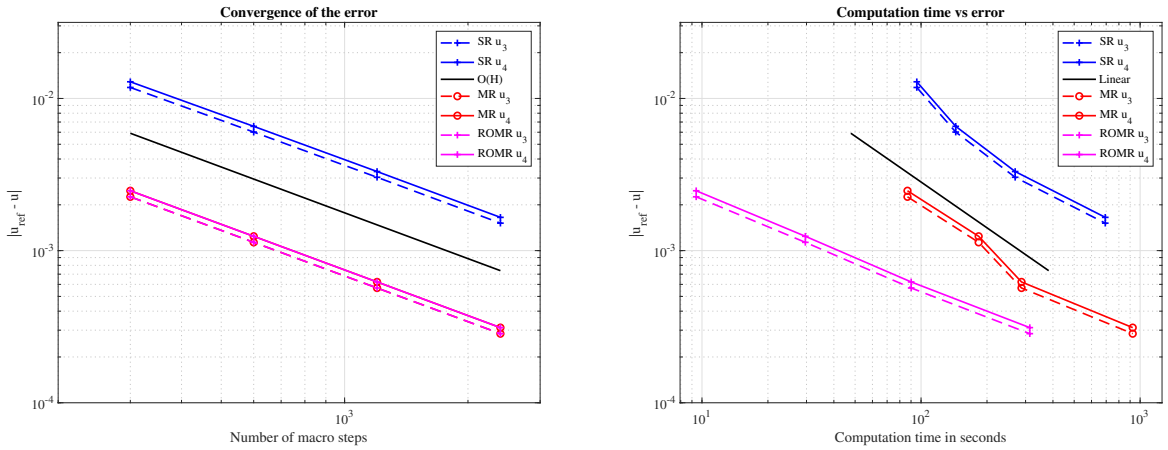

Figure 3: Convergence of the numerical schemes, where the error is plotted against the number of macro steps (left). Computational effort of the numerical schemes, where the error is plotted against the computation time in seconds (right). The error is defined as the absolute value between the computed voltage and reference voltage for each node.

Acknowledgements

The authors are indebted to the funding given by the European Union's Horizon 2020 research and innovation programme under the Marie Skłodowska-Curie Grant Agreement No. 765374, ROMSOC.

References

[1] C. Hachtel, J. Kerler-Back, A. Bartel, M. Günther, T. Stykel, Multirate DAE/ODE-simulation and model order reduction for coupled field-circuit systems, in: U. Langer, W. Amrhein, W. Zulehner (Eds.), Scientific Computing in Electrical Engineering - SCEE 2016. Book Series: Mathematics in Industry, Vol. 28, Springer, 2018, pp. 91–100., Springer, 2018.

[2] C. Hachtel, A. Bartel, M. Günther, A. Sandu, Multirate implicit Euler schemes for a class of differential–algebraic equations of index-1, J. Comput. Appl. Math. (2019) 112499.

[3] S. Chaturantabut, D. C. Sorensen, Nonlinear model reduction via discrete empirical interpolation, SIAM J. Sci. Comput. 32 (5) (2010) 2737–2764.

[4] Z. Drmac, S. Gugercin, A new selection operator for the Discrete Empirical Interpolation Method – improved a priori error bound and extensions, SIAM J. Sci. Comput. 38 (2) (2016) A631–A648.

[5] M. Günther, U. Feldmann, J. ter Maten, Modelling and discretization of circuit problems, HU. Langer, W. Amrhein, W. Zulehner (Eds.), Scientific Computing in Electrical Engineering - SCEE 2016. Book Series: Mathematics in Industry 28 (2018) 91–100.

[6] G. Berkooz, P. Holmes, J. L. Lumley, The proper orthogonal decomposition in the analysis of turbulent flows, Ann. Rev. Fluid Mech. 25 (1) (1993) 539–575.

[7] S. Chaturantabut, D. C. Sorensen, A state space error estimate for POD-DEIM nonlinear model reduction, SIAM J. Numer. Anal. 50 (1) (2012) 46–63.

[8] A. Bartel, M. Günther, M. Schulz, Modeling and discretization of a thermal-electric test circuit, in: K. Antreich, R. Bulirsch, A. Gilg, P. Rentrop (Eds.): Modeling, Simulation, and Optimization of Integrated Circuits, Springer, 2003, pp. 187–201.